J Mater Sci (2012) 47:7782–7788
DOI 10.1007/s10853-012-6587-8

ULTRAFINE GRAINED MATERIALS

Achieving homogeneity in a Cu–Zr alloy processed by high-pressure torsion

Jittraporn Wongsa-Ngam · Megumi Kawasaki · Terence G. Langdon

Received: 23 February 2012 / Accepted: 16 May 2012 / Published online: 30 May 2012

Abstract A copper alloy, Cu–0.1 %Zr, was subjected to severe plastic deformation at room temperature using quasi-constrained high-pressure torsion. Disks were strained through different numbers of revolutions up to a maximum of ten turns under an applied pressure of 6.0 GPa and then examined to evaluate the evolution in the Vickers microhardness, Hv, and the microstructure. The results show lower values of Hv in the center regions of the disks in the early stages of processing but a gradual evolution to a high degree of hardness homogeneity after five and ten turns. Under conditions of hardness homogeneity, the distributions of the grain boundary misorientations are essentially identical at the center and the periphery of the sample. Homogeneity was further confirmed by conducting tensile testing at elevated temperatures where similar stress–strain curves and similar elongations to failure were recorded after processing through five and ten turns of HPT.

Introduction

The fabrication of bulk ultrafine-grained (UFG) materials has become important because of the potential for producing materials having both high strength and a superplastic forming capability. These UFG metals may be produced through the application of severe plastic deformation as in processes such as equal-channel angular pressing (ECAP) [1] and high-pressure torsion (HPT) [2].

Extensive investigations of aluminum-based alloys showed that the addition of a small amount of zirconium restricts grain growth in UFG materials processed by ECAP and this provides an opportunity for achieving excellent superplastic properties with elongations up to >1000 % at elevated temperatures [3]. By contrast, there are only limited results showing the effect of adding Zr to Cu-based alloys. In earlier experiments, superplastic elongations were achieved in a Cu–30 %Zn–0.13 %Zr alloy processed by ECAP when testing in tension at 673 K but experiments on a Cu–0.18 %Zr alloy gave elongations to failure of <100 % [4]. The present investigation was initiated to evaluate the effect of a Zr addition on the properties of Cu after processing by HPT. This information is needed because it is well known that a Zr addition improves the fatigue properties of copper [5]. An earlier report described some of the preliminary results from this investigation [6] and this paper provides additional information on the microstructural evolution and the tensile properties. Specifically, the objectives of this investigation were to evaluate the characteristics of the microstructural development and to provide information on the mechanical properties of the alloy both at room temperature and at elevated temperatures after processing by HPT.

Experimental materials and procedures

The material used in these experiments was a commercial Cu151 alloy with a composition, in wt%, of Cu–0.1 %Zr.

J. Wongsa-Ngam (✉) · M. Kawasaki · T. G. Langdon
Departments of Aerospace and Mechanical Engineering and Materials Science, University of Southern California, Los Angeles, CA 90089-1453, USA
e-mail: wongsang@usc.edu

M. Kawasaki
Division of Materials Science and Engineering, Hanyang University, 17 Haengdang-dong, Seongdong-gu, Seoul 133-791, South Korea

T. G. Langdon
Materials Research Group, Faculty of Engineering and the Environment, University of Southampton, Southampton SO17 1BJ, UK

The alloy was received from Olin Brass (East Alton, IL, USA) in the form of a rolled strip with dimensions of 760 × 500 mm and a thickness of 1.5 mm. Disks for HPT, having diameters of 10 mm, were punched from the sheet and then polished to give a final thickness of ~0.83 mm. In the as-received condition, the mean linear intercept grain size was measured as ~20 μm with a slightly elongated grain structure due to the rolling.

All of the HPT processing was conducted under quasi-constrained conditions [2] using an HPT facility consisting of two massive upper and lower anvils having central depressions with diameters of 10 mm and depths of 0.25 mm. For HPT processing, a disk was placed in the central depression of the lower anvil, the anvil was then brought into a position so that a pressure was imposed on the disk and torsional straining was achieved by rotation of the lower anvil. This procedure was described in more detail in an earlier report [7] except that a lubricant was not placed around the edges of the depressions on the upper and lower anvils. All processing by HPT was conducted at room temperature (RT) using an applied load of 470 kN corresponding to an imposed pressure, P, of 6.0 GPa, a rotational speed for the lower anvil of 1 rpm and with different numbers of turns, N, ranging through 1/4, 1/2, 1, 3, 5, and 10 turns.

After HPT, each processed disk was mounted and carefully polished to a mirror-like surface in order to take microhardness measurements. These measurements were taken using an FM-1e microhardness tester equipped with a Vickers indenter using a load of 200 gf and a dwell time of 10 s. For each disk, the average microhardness values were measured along randomly selected diameters of each disk. These measurements were taken at intervals of 0.3 mm and at every point the average microhardness value was calculated from four separate points uniformly positioned around the selected position by a distance of 0.15 mm. The distance between adjacent indentations was at least three times the indentation size to avoid any interactions. The advantage of this procedure is that it provides the hardness values with a high degree of accuracy for each selected measurement point. The error bars were calculated at each point corresponding to the 95 % confidence limits. Additional hardness measurements were also taken over the total surface areas of each disk following a rectilinear grid pattern and the results from these measurements were presented earlier in the form of color-coded hardness maps [6].

Detailed microstructural analysis was conducted on sample processed through one and five turns using an electron-backscatter diffraction (EBSD) technique and orientation imaging microscopy (OIM). These observations were performed separately at the central and edge regions of the processed disks. The EBSD analysis was undertaken using a JSM 7001F scanning electron microscope (SEM) operating at an accelerating voltage of 15 kV and the EBSD patterns were collected with TSL OIM software at the center and edge regions: the step sizes were taken as 0.08 μm except at the center of the disk processed through one turn where the step size was 0.1 μm. The average grain sizes and the average misorientation angles of the grain boundaries were analyzed using this software in which high-angle grain boundaries (HAGBs) are defined as misorientations between adjacent measurement points of more than 15°. The clean-up procedure was performed in an OIM-TSL analyzer and included grain dilation (GD) with a grain tolerance angle (GTA) equal to 5° and a minimum grain size of 2 pixels and a grain confidence index standardization with a GTA of 5° and a minimum grain size of 2 pixels. The average confidence index of each condition was about 0.9 or more whereas the change of datum point was less than 10 % after the clean-up procedure. Average grain sizes were determined directly from the OIM images using more than 500 individual grains in each material.

To investigate the mechanical properties, tensile specimens were prepared from the disks both in the as-received condition and after processing through 1, 5, and 10 turns. Two miniature tensile specimens, having both gauge lengths and widths of 1 mm, were cut from each disk using electro-discharge machining (EDM). A schematic illustration of typical tensile specimens is given in another report [8]. To avoid any potential problems associated with microstructural inhomogeneities near the centers of the disks, these specimens were cut from two off-center positions on either side and equidistant from the center of each HPT disk. Earlier research showed that higher elongations are generally achieved in specimens machined from the off-center positions in HPT processing [9]. These tensile specimens were pulled to failure at temperatures of 673 and 723 K using an Instron testing machine operating at a constant rate of cross-head displacement and with initial strain rates from 1.0×10^{-4} to 1.0×10^{-2} s^{-1}.

Experimental results

Microhardness measurements after HPT

The values of the Vickers microhardness, Hv, are shown in Fig. 1 plotted as a function of the position within the disk: the lower dashed line denotes the hardness value of Hv ≈ 95 in the as-received condition prior to processing by HPT. These measurements demonstrate that the hardness increases significantly even after only 1/4 turn with a value of Hv ≈ 160 at the periphery of the disk but a much lower value of Hv ≈ 110 in the central region. Thereafter, there is little or no change in the hardness at the edge of the

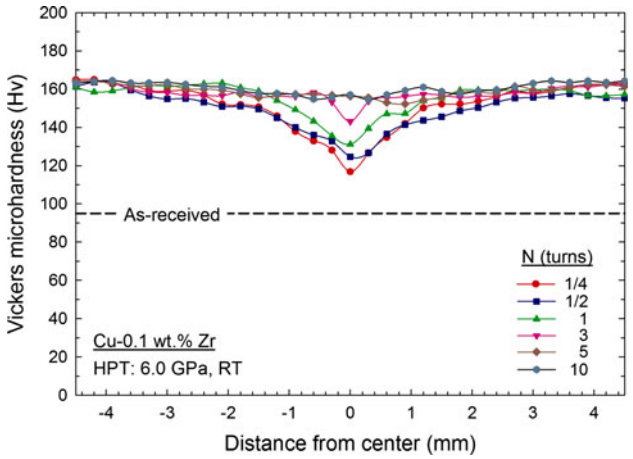

Fig. 1 Values of the Vickers microhardness versus distance from the center of the Cu–0.1 %Zr disks after HPT processing for various numbers of turns

disk but the hardness values recorded in the centers of the disks gradually increase with increasing numbers of turns and after five and ten turns there is essentially a hardness homogeneity with Hv $\approx$ 160 throughout each disk. This gradual development of hardness homogeneity is consistent both with other experimental reports for materials processed by HPT [10–18] and with strain gradient plasticity modeling of the HPT process [19].

Detailed information on the values of Hv and the associated error bars are summarized in Table 1 where the error bars denote the 95 % confidence limits based on the separate measurements recorded around each point. It is apparent from Table 1 that the error bars tend to be higher in the central region of the disk where initially there are significant inhomogeneities. However, the error bars in the central regions decrease with increasing torsional straining so that ultimately, after ten turns, the error bars are reasonably consistent across the disk diameter.

Microstructure after HPT processing

Figure 2 shows representative OIM images taken after (a) one turn and (b) five turns, where the upper row corresponds to the centers of the disks and the lower row corresponds to the peripheries: the individual colors correspond to different orientations of each grain as depicted in the unit triangle. Inspection of Fig. 2a reveals the inhomogeneous microstructure and elongated grains that are present after processing through one turn. Measurements showed the grain sizes were different in these two regions with an average grain size of $\sim$580 nm in the central region and $\sim$410 nm in the edge region. After five turns in Fig. 2b, the microstructure became very well-defined, the grains were more equiaxed and measurements gave average grain sizes of $\sim$500 nm at the center and $\sim$410 nm at the periphery. Thus, consistent with the hardness measurements shown in Fig. 1, the average grain size remains constant at the edge of the disk with additional HPT processing whereas the average grain size decreases in the central region.

Figure 3 shows the distributions of the misorientation angles of grain boundaries at the centers and edges of the

Table 1 Microhardness values along the radii of Cu–0.1 %Zr disks processed by HPT

Distance from center (mm)	Hv						
	No HPT	1/4 turn	1/2 turn	1 turn	3 turns	5 turns	10 turns
0.0	95.4 ± 1.7	116.8 ± 4.7	124.6 ± 5.1	131.0 ± 8.0	143.1 ± 4.8	156.2 ± 4.5	157.0 ± 1.8
0.3	95.5 ± 1.1	127.3 ± 5.0	129.7 ± 4.4	137.4 ± 4.9	153.4 ± 3.7	156.2 ± 2.4	155.1 ± 2.4
0.6	95.5 ± 1.4	133.8 ± 4.2	136.2 ± 2.0	145.1 ± 3.3	156.8 ± 2.4	155.0 ± 2.1	155.9 ± 2.0
0.9	95.6 ± 0.9	139.9 ± 2.7	140.6 ± 2.0	148.2 ± 2.7	156.2 ± 1.2	154.8 ± 2.5	158.1 ± 1.9
1.2	96.1 ± 1.2	148.0 ± 3.0	144.3 ± 1.4	154.0 ± 1.6	156.9 ± 0.4	155.6 ± 2.0	159.4 ± 1.3
1.5	96.3 ± 1.0	151.4 ± 1.9	147.5 ± 2.5	157.1 ± 1.9	156.4 ± 1.2	155.6 ± 1.1	158.3 ± 1.2
1.8	94.8 ± 1.1	152.0 ± 2.3	149.8 ± 1.2	160.1 ± 1.5	157.0 ± 2.3	157.9 ± 1.3	158.4 ± 1.7
2.1	95.5 ± 0.5	152.9 ± 1.5	150.5 ± 0.8	161.3 ± 1.7	156.4 ± 1.0	159.0 ± 1.0	160.0 ± 1.3
2.4	95.8 ± 1.0	156.5 ± 2.0	153.1 ± 1.8	161.2 ± 1.5	156.7 ± 0.8	159.0 ± 1.3	160.5 ± 2.0
2.7	94.7 ± 1.0	159.1 ± 1.1	155.1 ± 1.3	160.5 ± 1.7	157.4 ± 1.3	160.8 ± 1.0	161.9 ± 1.3
3.0	95.3 ± 0.8	158.3 ± 1.7	155.2 ± 0.5	160.5 ± 1.1	158.0 ± 1.1	161.0 ± 1.6	163.3 ± 0.9
3.3	95.9 ± 0.8	159.1 ± 2.5	156.4 ± 1.1	161.0 ± 1.6	159.3 ± 0.8	160.5 ± 2.5	163.8 ± 0.6
3.6	96.5 ± 0.9	161.4 ± 2.7	158.6 ± 1.5	159.9 ± 2.0	160.9 ± 1.6	161.4 ± 1.3	163.4 ± 1.3
3.9	96.5 ± 0.9	162.2 ± 2.2	160.0 ± 2.6	157.9 ± 2.2	162.1 ± 1.4	162.9 ± 1.6	164.4 ± 0.5
4.2	96.1 ± 1.4	163.8 ± 2.0	159.5 ± 3.3	157.4 ± 1.2	163.1 ± 1.0	163.2 ± 1.4	163.8 ± 1.2
4.5	95.9 ± 1.1	164.0 ± 2.5	159.3 ± 2.6	159.1 ± 1.6	163.3 ± 1.5	162.7 ± 2.3	163.6 ± 1.1

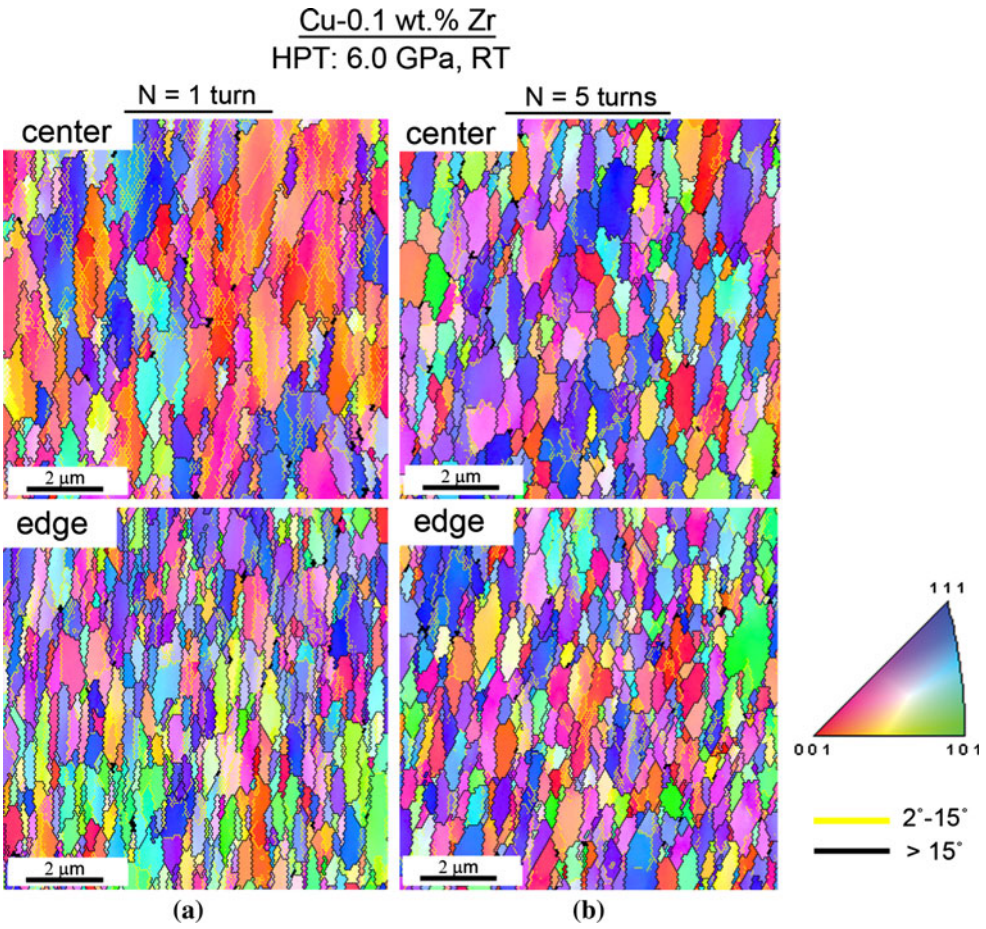

Fig. 2 EBSD orientation images of the Cu–0.1 %Zr disks processed by HPT for **a** one turn and **b** five turns; the *upper row* corresponds to the centers of the disks and the *lower row* corresponds to the edges of the disks

disks processed by HPT through (a) one turn and (b) five turns: information is given also for the total percentage of high-angle boundaries for each condition. These measurements show there is a relatively low fraction (46 %) of HAGBs in the center of the disk after HPT through one turn and this fraction is significantly higher (68 %) in the edge region. After five turns, as shown in Fig. 3b, the number fractions of grain boundary misorientations are essentially identical at both the center and the edge positions and measurements showed the percentages of HAGBs were 70 % at both positions.

Tensile properties at high temperatures

Figure 4 shows representative stress–strain curves for the specimens after HPT processing through one, five, and ten turns and in the as-received condition without HPT: these experiments were conducted using an initial strain rate of 1.0×10^{-3} s^{-1} at temperatures of (a) 673 and (b) 723 K. The plots show the Cu–Zr alloy exhibits typical high temperature behavior including little strain hardening and reasonable ductility. Detailed inspection of Fig. 4 shows the maximum yield stresses recorded after HPT for one turn are slightly lower than for the as-received material where this is attributed to the microstructural inhomogeneities produced in the early stages of torsional straining. Nevertheless, the yield strengths increase with increasing numbers of turns with the highest values recorded after five and ten turns. This is consistent with data reported for several materials processed by HPT including Fe [20] and an Al-7034 alloy [21].

The results in Fig. 4 demonstrate that, at a strain rate of 1.0×10^{-3} s^{-1}, the maximum elongations achieved in tension are ~175 % at 673 K and ~205 % at 723 K. However, to provide a more comprehensive display of tensile data over a range of strain rates, Fig. 5 plots the measured elongations to failure versus strain rate for samples in the as-received condition and after processing through one, five, and ten turns at (a) 673 and (b) 723 K. The results given in Fig. 5 cover initial strain rates from 1.0×10^{-4} to 1.0×10^{-2} s^{-1}, respectively.

Inspection of Fig. 5 leads to three important conclusions. First, the ductility increases significantly after HPT for five and ten turns whereas the samples processed through only one turn show similar elongations to specimens without HPT. This lower ductility in the samples after HPT for one turn is a direct consequence of the high

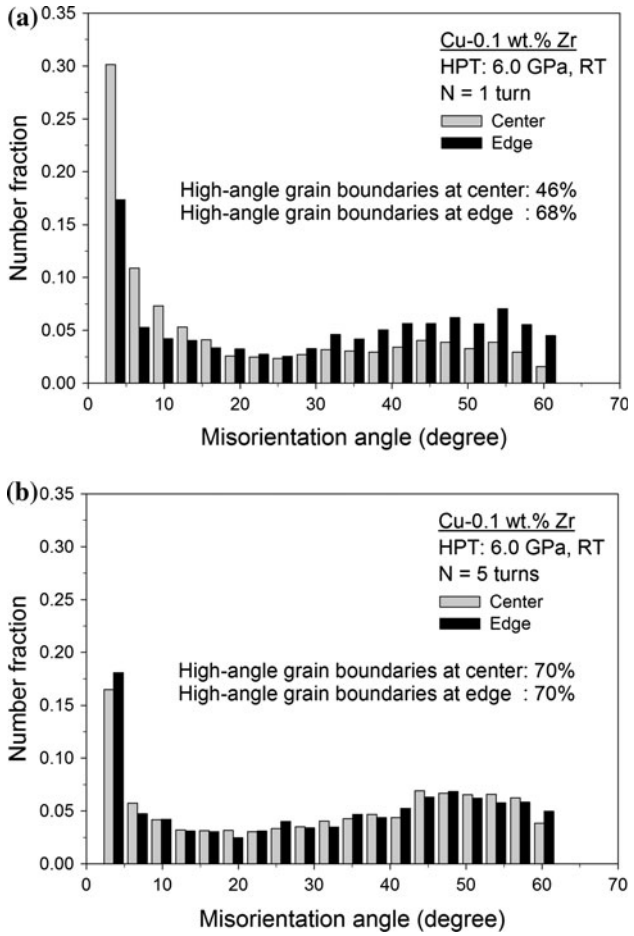

Fig. 3 Distributions of the number fraction of the misorientation angles of the grain boundaries at the centers and edges of the disks processed by HPT through **a** one turn and **b** five turns

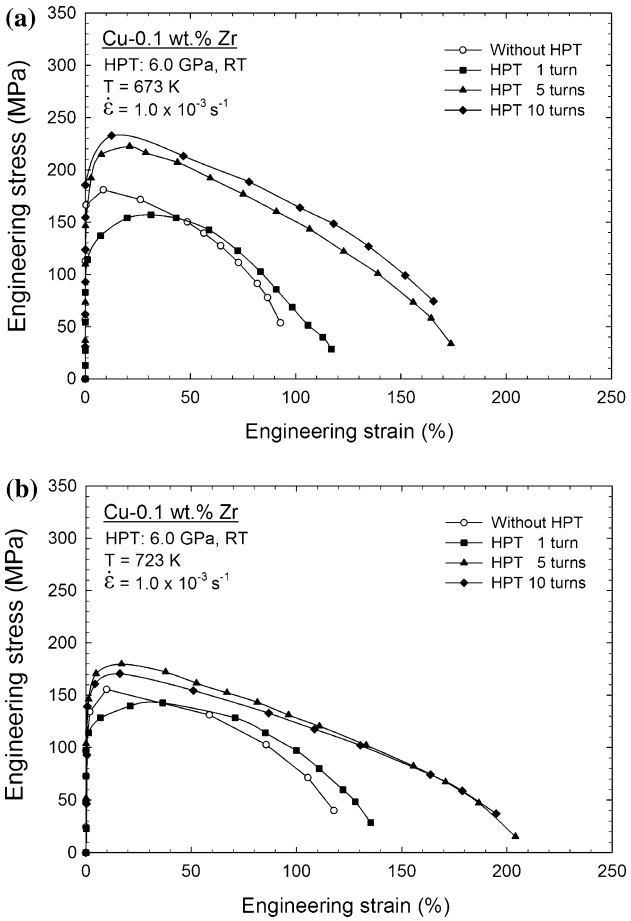

Fig. 4 Plots of engineering stress versus engineering strain for the Cu–0.1 %Zr alloy in an as-received specimen and after HPT processing through one, five, and ten turns at an initial strain rate of 1.0×10^{-3} s^{-1} and at temperatures of **a** 673 and **b** 723 K

degree of microstructural inhomogeneity as demonstrated earlier by the larger error bars associated with the hardness measurements in the early stages of HPT processing [6]. Second, after five and ten turns the measured elongations to failure consistently increase with decreasing strain rate and both processing conditions show almost identical results. The similarity between the samples processed through five and ten turns matches the hardness measurements shown in Fig. 1 where essentially identical hardness values are recorded after processing through five and ten turns. Furthermore, as in earlier experiments [11, 22–27], this confirms the close correlation between the hardness measurements and the microstructures produced by HPT. Third, the highest elongations recorded in these experiments were ~280 % for the two specimens processed through five and ten turns when testing at 723 K using a strain rate of 1.0×10^{-4} s^{-1}. This elongation does not fulfill the requirements for true superplastic flow where the measured elongation in tension should be at least 400 % [28].

Discussion

The results of this investigation show there is a gradual evolution toward hardness homogeneity across the disks of the Cu–0.1 %Zr alloy after five or more turns of HPT processing. This is consistent with earlier reports for pure Cu processed by HPT [12, 29–36] and for various Cu alloys [30, 31, 37, 38]. Several recent results on Cu alloys indicate also that the microstructural development in HPT processing is dependent upon the stacking fault energy of the alloy [39–43].

Using EBSD and OIM, the results in Fig. 2 provide a direct demonstration of the microstructural evolution that parallels the evolution in hardness: this evolution occurs both with additional torsional straining and between the center and edge of each HPT disk. It is important to note that the distributions of the grain boundary misorientation angles in Fig. 3b provide a direct confirmation of the microstructural homogeneity, in addition to the hardness homogeneity, that is attained after a relatively small

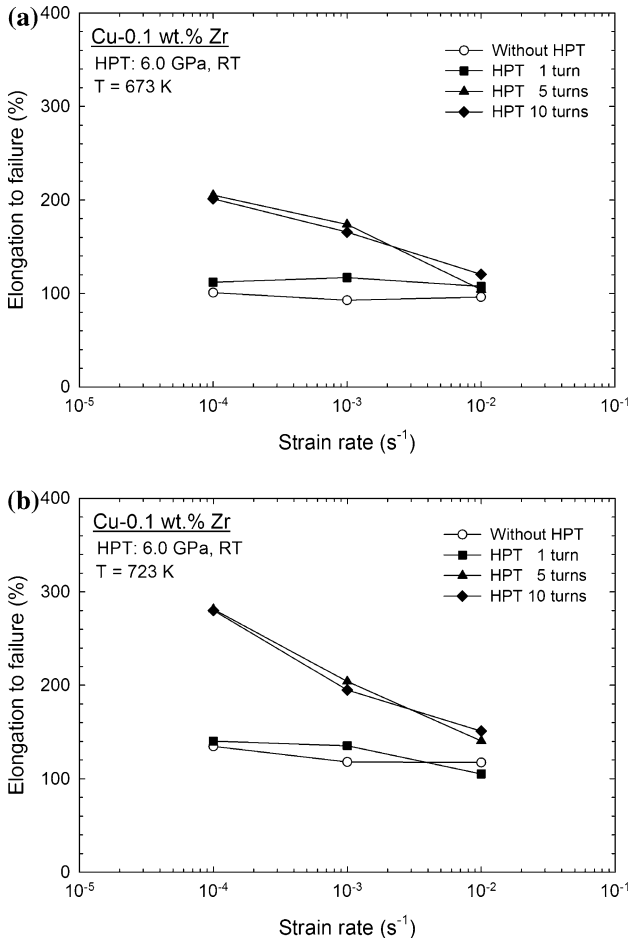

Fig. 5 Elongation to failure versus strain rate for the Cu–0.1 %Zr alloy in an as-received condition and after HPT processing through one, five, and ten turns and testing at temperatures of **a** 673 and **b** 723 K

number of turns. These results show, therefore, that HPT processing is especially effective in both refining the grains to the submicrometer level and in producing a homogeneous microstructure throughout each disk.

The equilibrium grain size recorded in this investigation was ~410 nm and this is larger than the grain sizes of ~310 nm at the center and ~180 nm at the edge of a disk for the same alloy processed by HPT through five turns when taking measurements using transmission electron microscopy (TEM) [6]. This difference arises because in practice lower grain sizes may be recorded using TEM both because of a tendency to directly measure the smaller grains and because of the limitations imposed in EBSD because of the size of the scanning step.

The results in Fig. 3b show that the percentage of HAGBs after five turns of HPT was about 70 % at both the center and the periphery of the disk. This is similar to the percentages of HAGBs recorded after processing by ECAP through a number of passes: for example, there are reports of 74 % of HAGBs in pure Al after 12 ECAP passes at room temperature [44] and 65 % of HAGBs in an Al–1 %Mg alloy after 8 ECAP passes at room temperature [45].

The highest elongations recorded in tensile testing in these experiments were only ~280 % after processing through five and ten turns and then testing in tension at 723 K. This elongation does not fulfill the requirement for superplastic flow which is defined as tensile elongations of at least 400 % and with measured strain rate sensitivities close to ~0.5 [28]. Nevertheless this value is significantly larger than the elongations of <100 % recorded for a Cu–0.18 %Zr alloy processed by ECAP and tested in tension at the lower temperature of 673 K [4]. It should be noted that the addition of a small amount of Zr increases the recrystallization temperature and inhibits grain growth [4] thereby leading to grain size stability at elevated temperatures. In practice, this grain stability may produce superior tensile properties such as high strength and reasonable tensile ductility.

In practice, it is now well-established that the ductilities achieved in tensile testing are dependent upon the dimensions of the tensile specimens [46, 47]. Specifically, higher elongations are achieved when using specimens with larger cross-sectional areas. In the present experiments, the tensile specimens had widths of 1 mm and thicknesses of <0.8 mm after HPT processing so that their cross-sectional areas were extremely small. This contributes in part to the relatively low elongations although it should be noted that a tensile elongation of ~1800 % was recorded recently in a tensile specimen cut from a highly superplastic Zn–22 %Al eutectoid alloy after processing by HPT [48]. More experiments are now needed to determine the requirements for achieving superplastic elongations in very dilute Cu-based alloys.

Summary and conclusions

1. Disks of a Cu–0.1 %Zr alloy were processed by quasi-constrained HPT through up to ten turns under an applied pressure of 6.0 GPa. Following HPT processing, the disks were examined to determine the evolution in hardness and microstructure with torsional straining and the tensile properties of the processed specimens at elevated temperatures.

2. The results show that homogeneity is achieved in this alloy after processing by HPT through five or more turns. This homogeneity is confirmed in three ways. First, hardness measurements show similar values across each disk after five or more turns. Second, the measured percentages of high-angle grain boundaries are identical in the center and at the edge of a disk processed for five turns. Third, tensile testing after HPT processing leads to similar

stress–strain curves and elongations to failure for samples processed through five and ten turns.

Acknowledgements This study was supported in part by the National Science Foundation of the United States under Grant no. DMR-0855009 and in part by the European Research Council under ERC Grant Agreement no. 267464-SPDMETALS.

References

1. Valiev RZ, Langdon TG (2006) Prog Mater Sci 51:881
2. Zhilyaev AP, Langdon TG (2008) Prog Mater Sci 53:893
3. Lee S, Berbon PB, Furukawa M, Horita Z, Nemoto M, Tsenev NK, Valiev RZ, Langdon TG (1999) Mater Sci Eng A272:63
4. Neishi K, Horita Z, Langdon TG (2003) Mater Sci Eng A352:129
5. Goto M, Han SZ, Kawagoishi N, Kim SS (2008) Mater Lett 62: 2832
6. Wongsa-Ngam J, Kawasaki M, Zhao Y, Langdon TG (2011) Mater Sci Eng A528:7715
7. Kawasaki M, Langdon TG (2008) Mater Sci Eng A498:341
8. Loucif A, Figueiredo RB, Kawasaki M, Baudin T, Brisset F, Chemam R, Langdon TG (2012) J Mater Sci. doi:10.1007/s10853-012-6400-8
9. Dobatkin SV, Bastarache EN, Sakai G, Fujita T, Horita Z, Langdon TG (2005) Mater Sci Eng A408:141
10. Vorhauer A, Pippan R (2004) Scripta Mater 51:921
11. Xu C, Horita Z, Langdon TG (2008) Acta Mater 56:5168
12. Edalati K, Fujioka T, Horita Z (2008) Mater Sci Eng A497:168
13. Edalati K, Fujioka T, Horita Z (2009) Mater Trans 50:44
14. Edalati K, Matsubara E, Horita Z (2009) Metall Mater Trans 40A:2079
15. Čížek J, Melikhova O, Janeček M, Srba O, Barnovská Z, Procházka I, Dobatkin S (2011) Scripta Mater 65:171
16. Loucif A, Figueiredo RB, Baudin T, Brisset F, Langdon TG (2010) Mater Sci Eng A527:4864
17. Kawasaki M, Alhajeri S, Xu C, Langdon TG (2011) Mater Sci Eng A529:345
18. Loucif A, Figueiredo RB, Baudin T, Brisset F, Chemam R, Langdon TG (2012) Mater Sci Eng A532:139
19. Estrin Y, Molotnikov A, Davies CHJ, Lapovok R (2008) J Mech Phys Solids 56:1186
20. Wetscher F, Vorhauer A, Pippan R (2005) Mater Sci Eng A410–411:213
21. Xu C, Dobatkin SV, Horita Z, Langdon TG (2009) Mater Sci Eng A500:170
22. Zhilyaev AP, Lee S, Nurislamova GV, Valiev RZ, Langdon TG (2001) Scripta Mater 44:2753
23. Zhilyaev AP, Oh-ishi K, Langdon TG, McNelley TR (2005) Mater Sci Eng A410–411:277
24. Xu C, Horita Z, Langdon TG (2007) Acta Mater 55:203
25. Zhilyaev AP, McNelley TR, Langdon TG (2007) J Mater Sci 42:1517. doi:10.1007/s10853-006-0628-0
26. Kawasaki M, Ahn B, Langdon TG (2010) J Mater Sci 45:4583. doi:10.1007/s10853-010-4420-9
27. Xu C, Horita Z, Langdon TG (2010) Mater Trans 51:2
28. Langdon TG (2009) J Mater Sci 44:5998. doi:10.1007/s10853-0093780-5
29. Horita Z, Langdon TG (2005) Mater Sci Eng A410–411:422
30. Ungár T, Balogh L, Zhu YT, Horita Z, Xu C, Langdon TG (2007) Mater Sci Eng A444:153
31. Balogh L, Ungár T, Zhao Y, Zhu YT, Horita Z, Xu C, Langdon TG (2008) Acta Mater 56:809
32. Lugo N, Llorca N, Cabrera JM, Horita Z (2008) Mater Sci Eng A477:366
33. Edalati K, Ito Y, Suehiro K, Horita Z (2009) Int J Mater Res 100:1668
34. Edalati K, Horita Z (2010) Mater Trans 51:1051
35. Edalati K, Horita Z (2010) J Mater Sci 45:4578
36. Čížek J, Janeček M, Srba O, Kužel R, Barnovská Z, Procházka I, Dobatkin S (2011) Acta Mater 59:2322
37. Jiang H, Zhu YT, Butt DP, Alexandrov IV, Lowe TC (2000) Mater Sci Eng A290:128
38. Tian YZ, Wu SD, Zhang ZF, Figueiredo RB, Gao N, Langdon TG (2011) Acta Mater 59:2783
39. Sun PL, Zhao YH, Cooley JC, Kassner ME, Horita Z, Langdon TG, Lavernia EJ, Zhu YT (2009) Mater Sci Eng A525:83
40. Wang YB, Liao XZ, Zhao YH, Lavernia EJ, Ringer SP, Horita Z, Langdon TG, Zhu YT (2010) Mater Sci Eng A527:4959
41. An XH, Lin QY, Wu SD, Zhang ZF, Figueiredo RB, Gao N, Langdon TG (2011) Scripta Mater 64:954
42. An XH, Lin QY, Wu SD, Zhang ZF, Figueiredo RB, Gao N, Langdon TG (2011) Phil Mag 91:3307
43. An XH, Wu SD, Zhang ZF, Figueiredo RB, Gao N, Langdon TG (2012) Scripta Mater 66:227
44. Kawasaki M, Horita Z, Langdon TG (2009) Mater Sci Eng A524:143
45. Xu C, Horita Z, Langdon TG (2011) Mater Sci Eng A528:6059
46. Zhao YH, Guo YZ, Wei Q, Dangelewicz AM, Xu C, Zhu YT, Langdon TG, Zhou YZ, Lavernia EJ (2008) Scripta Mater 59:627
47. Zhao YH, Guo YZ, Wei Q, Topping TD, Dangelewicz AM, Zhu YT, Langdon TG, Lavernia EJ (2009) Mater Sci Eng A525:68
48. Kawasaki M, Langdon TG (2011) Mater Sci Eng A528:6140